Int. J. Multiphase Flow, Vol. 4, pp. 117–140. Pergamon/Elsevier, 1978. Printed in Great Britain

THE EFFECTS OF COUNTERCURRENT SINGLE AND TWO-PHASE FLOWS ON THE QUENCHING RATE OF HOT SURFACES

R. B. DUFFEY,† M. C. ACKERMAN, B. D. G. PIGGOTT and S. A. FAIRBAIRN
Central Electricity Generating Board, Berkeley Nuclear Laboratories, Berkeley, Gloucestershire, England

(*Received* 20 *January* 1977)

Abstract—A theoretical and experimental study of liquid film flow and quench front propagation on hot vertical surfaces in the presence of single and two-phase upflows is reported. Experiments in which a water jet was used to cool a single rod set in a transparent tube showed that the downward progress of a quench front was significantly retarded or even stopped by an air or steam upflow. Climbing quench fronts were observed which sometimes coexisted with the falling quench fronts, but at surface temperatures above 900°C and flow rates below 0.9 g/s/cm both quench fronts became stationary. Conventional flooding correlations have been shown to overestimate the upflow necessary to cause flow reversal particularly at high surface temperatures. The analysis of film flow shows that a simple interfacial shear model, although incapable of describing the observed wave dynamics, can be used to correlate trends in the available data on rewetting and downcomer penetration. A preliminary theoretical examination of the wave dynamics at the onset of flow reversal is presented based on the Jeffreys theory of growth of finite-amplitude waves.

1. INTRODUCTION

We are interested in the rate of wetting of a hot vertical surface in the presence of a gas, steam or two-phase updraft. This problem has practical importance to the downward progression of quenching, due to the spray cooling or reflooding of over-heated water reactor fuel bundles, and to the penetration of emergency cooling water in vertical downcomers or pipes. The updraft or counterflow may be steam from boiling and evaporation of the liquid film itself on the hot surfaces, or single or two-phase flows derived by water boiling because of reactor depressurisation.

It is known that interactions occur between a water downflow and the gas upflow (a so-called "countercurrent flow"), causing waves to grow on the water surface, and the downflow may be stopped or even reversed by the interchange of momentum, a phenomenon known as "flooding" (Hewitt & Wallis 1963; Wallis 1969; Duncan & Leonard 1971; Naff & Whitbeck 1972; Shires *et al.* 1964). Identical situations occur in chemical plants in the "flooding" or flow reversal of packed beds or wetted wall columns (Wallis 1969; Shearer & Davidson 1965; Nicklin & Davidson 1969), and simplified correlations to describe the steady-state flooding point of no net downflow have been developed (Wallis 1969; Wallis & Makkenchery, 1974; Grolmes *et al.* 1974). If upward liquid flow results from high counterflows (so-called "co-current flow") and the walls can be wetted, the flow pattern may become annular, a regime of great interest in two-phase flow analysis (Hewitt & Hall-Taylor 1970). Counterflow effects are also important in estimates of dryout in reactors and heat exchangers when the conditions for the disappearance of the boiling liquid film are required (Whalley *et al.* 1974), and in studies of the motion of molten cladding in postulated accidents for fast reactors (Theofanous *et al.* 1976).

When the surface is hot (≥ 300°C) thermal conduction within the surface controls the rate of progression of the rewetting front and the liquid film down the walls, and steam and drops are generated by the boiling at the front (Duffey & Porthouse 1972, 1973). If the steam production and droplet evaporation are sufficient, reversal of the liquid film flow or "flooding" might be expected (Chan & Grolmes 1975). Defining this reversal is obviously important, but no direct information is currently available on the liquid film flow on high temperature surfaces in the presence of single and two-phase counterflows. Detailed studies of the hydrodynamics and wave formation at the onset of flow reversal are also not available.

†Present address: Electric Power Research Institute, 3412 Hillview Avenue, Palo Alto, CA 94303, U.S.A.

This paper examines the analysis of transient liquid film flow and wave formation in countercurrent flows, and the effect of boiling and thermal conduction on the phenomena. New data are reported on the retardation and onset of flow reversal of a falling liquid film on a hot vertical cylinder, and the conditions for the generation of a climbing rewetting front determined.

2. THEORETICAL CONSIDERATIONS

A large body of literature is available on the hydrodynamics of liquid films and we first review some of the relevant physical considerations. From these, we outline an approximate analysis of film flow on hot surfaces and then the dynamics of wave growth on thin films is briefly examined. Both these analyses are extensions of previous work.

2.1 *General remarks*

Consider water running down a hot surface in the presence of a counterflow (figure 1a). Clearly the problem involves both the hydrodynamics of liquid film flow and the thermal phenomena involved in boiling and rewetting, neither of which are completely understood at the present time. The hydrodynamics involve, firstly, the stability of thin film flows, since the film can support both surface-tension dominated ripples and gravity waves of longer wavelength and it has been shown that the surface is always unstable with respect to infinitesimal disturbances (Benjamin 1957; Yih 1963; Lee 1969). Secondly, the interfacial shear due to the countercurrent flow distorts the velocity profile within the liquid from the classic Nusselt parabolic profile due

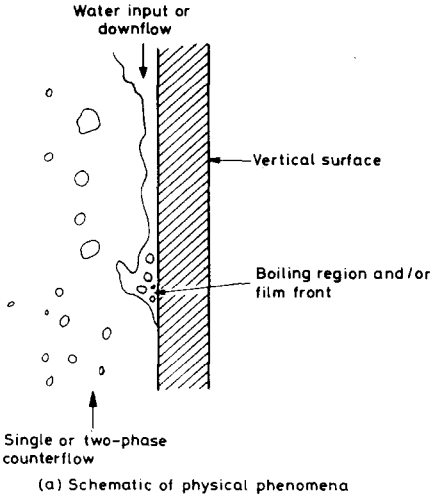

(a) Schematic of physical phenomena

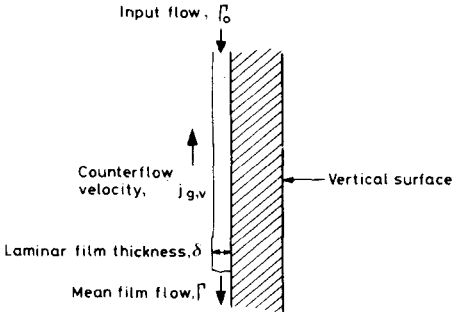

(b) Idealisation for interfacial shear analysis

Figure 1. Conditions at the interface.

to the wall shear, causing the gas–liquid interface velocity to decrease while the mean flow is downward (Hewitt & Wallis 1963; Grolmes *et al.* 1974). Thirdly, the counterflow causes the growth of waves on the surface (Hanratty & Hershman 1961; Hewitt & Wallis 1963; Shearer & Davidson 1965; Centinbudaklar & Jameson 1969; Gottifredi & Jameson 1970), this being a particular case of the classic problem of wave generation due to wind over water (Jeffreys 1925*a*, *b*; Miles 1957, 1967; Barnett & Kenyon 1975).

The occurrence and characteristics of large two-dimensional waves (so-called "roll" or "disturbance" waves) in thin films has been and is the subject of intensive study (see, e.g. Lacey *et al.* 1962; van Rossum 1959; Miya *et al.* 1971; Telles & Dukler 1970; Chu & Dukler 1974, 1975; Ueda & Tanaka 1974; Ueda & Nose 1974). These aperiodic waves are important not only because the onset of flow reversal has been reported as due to waves growing in the liquid and bridging or blocking the flow area (Centinbudaklar & Jameson 1969; Hewitt & Wallis 1963), but also because the pressure drop is affected by the roughened surface presented by the waves to the flow (Anderson & Mantzouranis 1960; Hewitt & Wallis 1963; Dukler 1972). In addition, the majority of the liquid mass flow ($\sim 90\%$) can be transported by these waves moving over the thin liquid layer, or substrate, left on the wall (Chu & Dukler 1974). The wave growth is primarily a local phenomenon, the driving force being due to the pressure variations over the wavy surface and flow separation on the leeward side (Shearer & Davidson 1965; Jeffreys 1925*a*, *b*). The wave shape and velocity are dependent on local conditions because the waves are of finite height on a thin liquid layer and hence cannot travel without change of form (Lamb 1945; Landau & Lifschitz 1959; Chu & Dukler 1974). The wave crest becomes steeper and may be eroded or entrained by the counterflow as a spray (Mayer 1961; Ishii & Grolmes 1975) or as a plug of liquid in a small channel (Nicklin & Davidson 1962; Wallis & Dobson 1973).

The thermal phenomena further complicate the picture, since the water film may be boiling. The rate of advance of the liquid over a hot surface in the absence of counterflow, u_0, is known to be controlled by thermal conduction within the surface, with a clear "rewetting front" characterised by violent boiling at the edge (Shires *et al.* 1964; Duffey & Porthouse 1972, 1973) which thickens and disrupts the liquid film. The rewetting rate is now known to be a function of the local water flowrate per unit heated perimeter, Γ, and the subcooling, ΔT_s (Yoshioka & Hasegawa 1970; Piggott & Porthouse 1973, 1975; Yu 1977), as well as being influenced by the thermal properties and thickness of the surface and any underlying material (Semeria & Martinet 1965; Piggott & Duffey 1975; Pearson *et al.* 1977). The functional dependency of the non-dimensional rewetting velocity without counterflow, u_0^*, may be stated as

$$u_0^* = \frac{\rho c \epsilon u_0}{k} = u_0^*(\Gamma, \Delta T_s, T_w, T_q, (kpc)_u,) \qquad [1]$$

where ρ, c and k are density, specific heat and thermal conductivity of the surface material and ϵ its thickness, the subscript u refers to the underlying or filler material. T denotes temperature, the subscript w referring to the upstream wall or surface value and q to the value at the quench front, i.e. T_q is a "Leidenfrost" or rewetting temperature.

If the counterflow reduces the film flowrate, then the rewetting rate should reduce. Because kinetics of the boiling process are not well understood, it is not known what "correct" value to apply to T_q, e.g. proposals include the minimum wall temperature for film boiling, or the wall temperature at the breakdown of nucleate boiling at the "critical heat flux". Nevertheless data for a wide range of surfaces and conditions have been simply correlated (Yu 1975; Piggott & Porthouse 1975).

An exact solution is not available for the counterflow-induced growth of an orbitrary-shaped wave on a boiling thin liquid layer falling on a vertical surface in the presence of steep local wall temperature gradients. Even simple cases present difficulties, and some simplifying concepts must be applied. The following sections consider such special cases.

2.2 *Modified laminar film analysis with interfacial shear*

It is known that the generation of waves determines the point of flow reversal (Hewitt & Wallis 1963). The initial gross approximation is to neglect the surface waves, as shown in figure 1b, and treat the liquid film as smooth with an interfacial shear due to countercurrent flow (Grolmes *et al.* 1974). The effect of the waves on the shear and film flowrate can then be corrected for using a dimensionless multiplier, f, which may or may not be related to the conventional two-phase pressure drop multiplier. This approach is supported by indirect measurements which show that the mean film thickness, δ, is relatively unaffected by counterflow up to the point of "flooding" (Nicklin & Davidson 1962; Anderson & Mantzouranis 1960; Lacey *et al.* 1962; Hewitt & Wallis 1963) and may nearly be given by the Nusselt expression,

$$\delta_0 = \left(\frac{3\mu_L \Gamma_0}{g\rho_L^2}\right)^{1/3} \qquad [2]$$

where μ is viscosity and g gravitational acceleration, the subscripts L and 0 refer to liquid and input or initial value. However, the velocity profile across the film is distorted by the shear, and with the above approximations, the mean film flowrate is, recasting the equation derived by Hewitt & Wallis (1963) and later by Grolmes *et al.* (1974),

$$\Gamma = \Gamma_0\left[1 - 0.25\left(\frac{g^2\rho_L\mu_L\Gamma_0}{9}\right)^{-1/3} f\bar{\rho}j^2\right]. \qquad [3]$$

Here Γ_0 is the input flowrate, j is the local relative interphase velocity and $\bar{\rho}$ the mean counterflow density. This equation has been used with the condition $\Gamma = 0$ to correlate a range of "flooding" data in smooth heated and unheated tubes using f as an arbitrary parameter (Grolmes *et al.* 1974; Chan & Grolmes 1975): no general test of its ability to correlate film flow information has however been made. Now, from [1], the rewetting rate at constant subcooling may be expressed empirically as,

$$u_0^* \propto \Gamma^m \qquad [4]$$

where m varies from about 0.3 for low flowrates and/or nearly saturated water, to unity for subcooled water (Piggott & Porthouse 1975; Yu 1977). Substituting [4] in [3], gives

$$u^* = u_0^*\left[1 - 0.25\left(\frac{g^2\rho_L\mu_L\Gamma_0}{9}\right)^{-1/3} f\bar{\rho}j^2\right]^m \qquad [5]$$

where u^* is the non-dimensional rewetting velocity with counterflow. Note that variations in rewetting velocity due to heater properties, etc. are taken into account by the use of u_0^*. The effect of shear due to counterflow is to reduce the rewetting rate and the limits of [5] are

$$u^* \to u_0^*, \quad \text{as} \quad \Gamma_0 \to \infty \quad \text{or} \quad j \to 0 \qquad [6.1]$$

and

$$u^* \to 0, \quad \text{as} \quad j = j_f \to \frac{2(\rho_L g^2 \mu_L)^{1/6}}{9^{1/6}(\bar{\rho}f)^{1/2}}\Gamma_0^{1/6} \qquad [6.2]$$

where the subscript f refers to the value at onset of flow reversal or flooding. Equation [6.2] is the Chan & Grolmes (1975) "hydrodynamically controlled" condition. For air or steam at atmospheric pressure blowing over a water film, as an order of magnitude,

$$j_f \simeq 24\,\Gamma_0^{1/6} \text{ m/s with } \Gamma_0 \text{ in g/s/cm}$$

and $f \simeq 0.006$ the smooth tube value.

2.3 *Effect of steam generation on the top spraying and flooding of hot channels*

The conditions encountered in some emergency cooling experiments on the spraying and flooding of hot channels and pin bundles (Duncan & Leonard 1971; Blaisdell *et al.* 1973; Griebe & McConnell 1973; Guerrero & Lowe 1974) are such that the upflow is due to evaporation of the injected water itself. The vapour flow can then be such as to cause "flooding" thus limiting the inflow of water into the hot channel (Shires *et al.* 1964; Chan & Grolmes 1975). The theory of section 2.2 can be simply extended for this situation; this is required because it is distinct from the case of a superimposed upflow. We need an expression for steam generation rate to substitute for $\bar{\rho}j^2$ in [3]. This presents some difficulties since the exact mechanism of steam generation is not known. So for a wetted perimeter, p, and a flow area A, the appropriate mass balance is assumed to be

$$\rho_v j_v A = \alpha p(\Gamma_0 - \Gamma) \qquad [7]$$

where α is a constant of proportionality and the subscript v denotes vapour. It has also been assumed that the liquid film thickness is small compared with the equivalent diameter thus j_v is based on the full flow area. Substituting for $\rho_v j_v^2$ from [7] in [3] gives

$$1 - \frac{\Gamma}{\Gamma_0} = \frac{4A^2\rho_v}{\alpha^2 f p^2}\left(\frac{g^2\rho_L\mu_L}{9}\right)^{1/3}\Gamma_0^{-5/3} \qquad [8]$$

and, from [4] yields,

$$1 - (u^*/u_0^*)^{1/m} = \frac{4A^2\rho_v}{\alpha^2 f p^2}\left(\frac{g^2\rho_L\mu_L}{9}\right)^{1/3}\Gamma_0^{-5/3}. \qquad [9]$$

Equations [8] and [9] are the general equations for the film flowrate and rewetting velocity on hot surfaces. Note that the limits of [9] are, firstly,

$$u^* \to u_0^* \quad \text{as} \quad \Gamma_0 \to \infty, \qquad [10.1]$$

i.e. at high input flows, the progress is purely conduction controlled; this limit was also stated by Chan & Grolmes (1975) who argued that there was insufficient droplet evaporation by radiation absorption to produce sufficient steam for flow reversal. Secondly,

$$u^* \to 0 \quad \text{when} \quad \Gamma_0 = \Gamma_{0f} \to \left(\frac{4A^2\rho_v}{\alpha^2 f p^2}\right)^{3/5}\left(\frac{g^2\rho_L\mu_L}{9}\right)^{1/5} \qquad [10.2]$$

so that at some critical input flow, Γ_{0f}, the downward flow is arrested completely, as for the case of a superimposed upflow [6.2].

Experimental data are scarce, and only the preliminary results of Guerrero & Lowe (1974) are available for comparison; they poured 20°C water into a 4 m long tube at 800°C, and measured the quenching times. The data are compared with theory in figure 2, where for the purposes of comparison and since $m \simeq 1$ for this case, [9] has been simply recast as,

$$1 - (t_{q0}/t_q) = \frac{4A^2\rho_v}{\alpha^2 f p^2}\left(\frac{g^2\rho_L\mu_L}{9}\right)^{1/3}\Gamma_0^{-5/3} \qquad [11]$$

$$= K\Gamma_0^{-5/3}, \quad \text{say}, \qquad [12]$$

where t_q is the measured quench time and t_{q0} is strictly the quench time with zero counterflow.

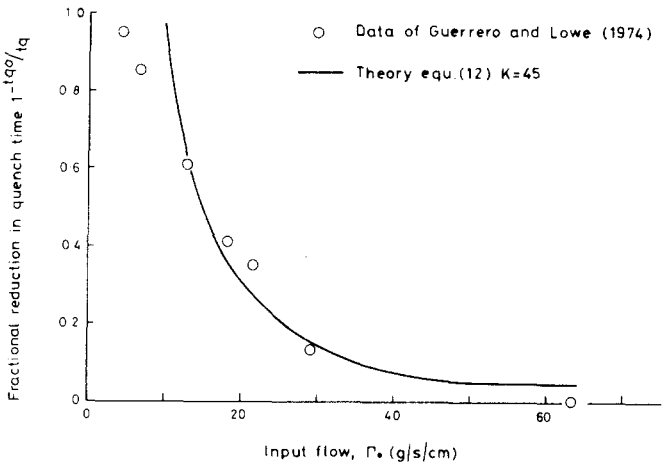

Figure 2. Comparison of interfacial shear analysis with top flooding data.

The value of t_{q0} is not known and has therefore been taken as the asymptotic quench time of [10.1] at the highest flowrate tested. K is partly empirical since the interfacial shear and α are unknown. Despite the data scatter, the agreement in the trends of quench time with flowrate lends some credibility to the above arguments.

2.4 *The dynamics of counterflow-induced waves of finite height on thin water films*

The preceding analysis is for a smooth interface, and has no implicit treatment of surface waves except by arbitrary manipulation of f. But, as stated above, waves are known to occur at the flooding point on falling water films and in annular flow. Chu & Dukler (1974) have emphasised that the statistical characteristics of finite waves must be considered, and that small perturbation analysis (e.g. of Yih 1963) will not suffice. In addition, the wave development is a transient process, so "standing wave" treatments are only a first approximation (see e.g. Shearer & Davidson 1965).

The simplest form of treatment of finite-amplitude wave growth on a water surface is the Jeffreys' "sheltering" model (Jeffreys 1925*a*, *b*). In this theory, the energy input to the waves is assumed proportional to the dynamic pressure, $\rho_g j_g^2$ (the subscript g refers to gas), which may be considered as due to flow separation in the lee of the wave (c.f. flow over a rib), as shown by Shearer & Davidson (1965). This model can be applied to irrotational flows, and hence to finite waves on a substrate or liquid layer of thickness, δ_B, such that (Lamb 1945),

$$\delta_{B_{\min}} \simeq 2\pi \left(\frac{2\mu_L \lambda}{\rho_L v}\right) \qquad [13]$$

where v is the wave celerity and λ the wavelength. With these approximations, balancing the rate of change of wave kinetic energy with the loss due to viscous dissipation and the gain due to wind pressure (Lamb 1945; Jeffreys 1925*b*) gives the equation for the local wave amplitude in a thin liquid layer as,

$$\frac{dh}{dt} = \left[\frac{\beta \rho_g (j_g - v)^2}{2\rho_L v \delta_B} - \frac{2\mu_L}{\rho_L}\frac{4\pi^2}{\lambda^2}\right] h \qquad [14]$$

where h is the wave height and β is the sheltering parameter. Following Jeffreys (1925*b*) and also Mayer (1961) who used the deep water form of the theory when $\delta \gg \lambda$ to examine entrainment from the crests of capillary waves, we note that the necessary and sufficient conditions for the wave to grow is that the R.H.S. of [14] should be positive, or otherwise the

wave decays due to viscous dissipation. This consideration gives the growth or neutral stability criterion for the minimum wave length, λ_m, or gas velocity, j_{gm}. Since the waves on falling films are gravity-controlled (Jeffreys 1925*b*; Telles & Dukler 1970), we consider two possible wave celerities as follows.

(a) For long gravity waves with $v \simeq (gh)^{1/2}$ in a liquid of depth $> \delta_{B_{\min}}$, from [14] for $(dh/dt) > 0$,

$$\lambda_m^2 \geq \frac{16\pi^2 \mu_L \delta_B}{\beta \rho_g j_g^2} (gh)^{1/2} \qquad [15]$$

and, neglecting viscous dissipation,

$$h^{1/2} - h_0^{1/2} = \left(\frac{\beta \rho_g j_g^2}{4\rho_L \delta_B}\right) \frac{t}{g^{1/2}} \qquad [16]$$

where h_0 is the original height at time $t = 0$, and we have used the fact that $j_g \gg v$.

(b) For Yih–Benjamin or finite-amplitude Kapitza waves (Lee 1969) predicted to occur on a thin draining film with $v \simeq (gh^2/\nu_L)$, ν being kinematic viscosity, from [14] for $(dh/dt) > 0$,

$$\lambda_m^2 \geq \frac{16\pi^2 g \rho_L \delta_B}{\beta \rho_g j_g^2} h^2 \qquad [17]$$

and, neglecting viscous dissipation,

$$h^2 - h_0^2 = \left(\frac{\beta \rho_g j_g^2}{\rho_L \delta_B}\right) \frac{\nu_L}{g} t. \qquad [18]$$

Note the restriction that λ_m must be large enough to satisfy [15] or [17], but not so large as to suffer dissipation by violating the irrotational flow requirement for δ_B (see Jeffreys 1925b).

Typical values for λ_m for water are $\sim 10^{-1}$ cm for (a) and (b) with $\beta \sim 0.3$–0.5 (Jeffreys, 1925*a*; Shearer & Davidson 1965), $j_g \sim 1$ m/s, and $\delta_B \sim h \sim 10^{-1}$ mm, and hence visual observations of the wave growth are a critical test of the controlling parameters. The mean wave height, $\bar{h}$, may be defined conventionally as

$$\bar{h} = \frac{v}{\lambda} \int_0^{\lambda/v} h \, dt \qquad [19]$$

and is evidently a function of time. From [16], $h \alpha j_g^4$, a result consistent with the observations of Ueda & Tanaka (1974) on wave growth on thin films just before the onset of crest entrainment or atomisation and for the film flow Reynolds number $(4\Gamma/\mu)$ of $\lesssim 2000$ of interest to the present work.

2.5 *Wave growth and the onset of bridging*

An alternative model is now considered; all the film flow, Γ, is assumed to develop a two-dimensional wave on the liquid film, the wave being held stationary by the counterflow. The wave, of width a, grows in height up to the point of bridging, i.e. for $h < R - r$, R and r being outer and inner radii of an annulus,

$$\rho_L a \frac{dh}{dt} \simeq \Gamma. \qquad [20]$$

Assuming the width to be determined by the wavelength of a wave formed by wind blowing

over water, then

$$a = 0[\lambda] = n\lambda, \quad \text{say,} \tag{21}$$

where n is an integer and the growth is given by,

$$\frac{dh}{dt} = (\Gamma/n\rho_L\lambda). \tag{22}$$

As an estimate, the value of λ can be taken from the results of different approximations (e.g. above, or Hanratty & Hershman 1961).

$$\text{Note} \quad j_g = j_{gs}\left(1 - \frac{h}{R-r}\right)^{-1}, \quad \text{from geometry} \tag{23}$$

and where the subscript s denotes the superfical value based on the full flow area and,

$$\Gamma = \Gamma_0\left[1 - 0.25\left(\frac{\rho_L g^2 \mu_L}{9}\right)^{-1/3} \Gamma_0^{1/3} \rho_{g,v} f j_{g,v}^2\right] \text{ from above.}$$

Hence from [22],

$$\frac{dh}{dt} = \frac{\Gamma_0}{\rho_L \lambda n}[1 - 0.25(\rho_L g^2 \mu_L)^{-1/3} \Gamma_0^{-1/3} \rho_{g,v} f j_{g,v}^2]. \tag{24}$$

Following "bridging", the plug of liquid formed could be accelerated upwards due to the dynamic pressure of the counterflow. For the acceleration from rest of a simple liquid column of length, l, integrating the momentum equation gives the vertical position, z, neglecting wall shear, as,

$$z = \frac{\beta \rho_g j_g^2}{2\rho_L l} t^2. \tag{25}$$

The above considerations all suggest that observations of film flow, wave growth rates and plug motion are important. Ideally, the effective interfacial shear parameter, f, should be related to the wave dynamics; because the wave height is time-varying, no simple relationship is immediately available.

3. EXPERIMENTS

The object of the experimental work was to check the above theories by investigating the effect of air, steam and two-phase steam/water counterflows on the falling film quenching of a heated rod at atmospheric pressure. The purpose of the air experiments was to examine momentum interchange phenomena, and that of the steam flow experiments to quantify the additional effects of counterflow density and condensation. The two-phase experiments, though more difficult to interpret, provide a useful indication of the additional phenomena which may occur in the blowdown and reflooding of water reactors, and are also relevant to simultaneous spraying and flooding by emergency core-cooling systems. Simple single pin experiments were adopted as being the more readily interpreted, with annular flow areas similar to current nuclear reactor values.

3.1 *Description of apparatus*

The test section for most experiments consisted of a heated rod of 14.2 mm o.d. located centrally within a smooth transparent silica tube of 19.5 mm bore (figure 3). Some additional scoping experiments were performed in a wider bore tube. The heater had a 347 stainless steel cladding 0.64 mm thick and was heated by a resistance element in a boron nitride filler; the heated length was 450 mm. Five 1 mm o.d. stainless steel sheathed thermocouples were positioned under the cladding of the heater in a line at approx. 76 mm intervals along the heated length. These internal thermocouple readings were monitored on ultra-violet and pen recorders. Demineralised water from a heated constant-head tank was supplied as a jet at normal incidence to the heater via a capillary tube set in the silica tube wall. The rod was positioned in the tube so that one of the internal thermocouples was directly beneath the point of jet impact. The two-phase counterflow was produced by allowing the test section to reflood from the bottom; the carryover from the quench front thus produced was a saturated two-phase mixture estimated to have a quality $\neq 1\%$. The water feeding the bottom quench front was arranged in separate experiments to come either from that injected onto the heater or from an independent supply, or from both.

3.2 *Experimental procedure*

For single-phase counterflow experiments the procedure was as follows. The required counterflow of air or steam was first set up and the temperature of the test section set to the

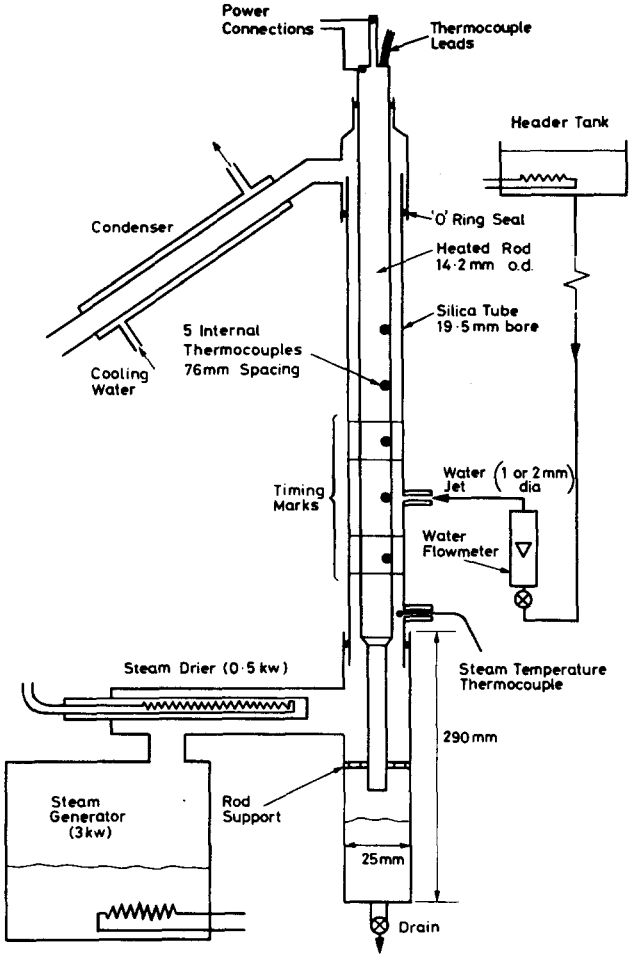

Figure 3. Steam counterflow apparatus—schematic.

desired initial value as indicated by the thermocouple located at the position of water jet injection. (There was an axial temperature difference due to the counterflow of approx. 100°C at maximum flow.) The water header tank was heated to the desired temperature. The rig was then allowed to stand for some minutes in order to achieve thermal equilibrium. To initiate a test, the water jet was turned on and the vertical progression of the quench fronts was measured by stopwatch timings between markers on the silica tube 50 mm and 100 mm from the jet. The signals from the internal thermocouples, one at the jet location, one 76 mm below and one 152 mm above it, and the water temperature were monitored on a chart-recorder. When spraying the rod with hot water, certain conditions of initial temperature and counterflow caused an unacceptably long wetting delay due to film boiling (Piggott *et al.* 1976). Wetting was initiated in these cases by momentarily increasing the jet flow and/or injection of cold water from an auxiliary supply: this did not significantly affect the subsequent behaviour.

The following range of conditions were investigated:

Rod initial temperature	300 – 1000°C	(± 10°C);
Jet flow	1 – 8 g/s	(± 0.1 g/s);
Steam velocity	0 – 15 m/s	(± 0.3 m/s);
Air velocity	0 – 12 m/s	(± 0.3 m/s);
Water temperature at jet	20 – 85°C	(± 2°C).

The conditions of film flow disruption (onset of plug flow) and of no net downflow were also determined with the rod cold. For the low jet flow, high counterflow experiments, the capillary jet size was reduced from 2 mm to 1 mm bore otherwise jet entrainment occurred.

The powers to maintain the initial steady-state temperatures in the absence of water injection are summarised in table 1 below. The power levels were lower for the steam experiments, when the silica tube was not water cooled to minimise condensation.

Table 1. Heater power levels to maintain steady initial temperatures

		Power (W)	
T_w(°C)	Counterflow	$j_{v,g} = 0$	$j_{v,g} = 15$ m/s
500	Air	620	1010
500	Steam	300	630
700	Air	1120	1710
700	Steam	700	1220
700	Two-phase	800	—
900	Air	2140	2690
900	Steam	1550	2280

For the two-phase counterflow experiments, it was not possible to maintain a steady counterflow as in the steam and air experiments. The heater power required to maintain a given surface temperature in the presence of counterflow could not be determined accurately. The method adopted was therefore to start the jet flow just as the bottom-flood water quenched the lower end of the heated length of the heater and then to increase the power to the heater in order to maintain constant the surface temperature, as recorded at a point about 150 mm above the level of the jet.

3.3 *Visual observations in single-phase counterflow*

At conditions of zero or low counterflow (< 1 m/s) the heater was quenched by a falling film in the form of a rivulet for cold water, or as a circumferentially uniform front for hot water. As counter flow velocity was increased the quench front velocity reduced and the quench front tended to become circumferentially uniform. At even higher velocities, waves formed at the quench front which nearly always bridged the annulus to form plugs of water which were

accelerated upwards by the counterflow and eventually disintegrated. A climbing film was also formed which appeared to obtain its flow from the passage of these plugs and after the plug had passed the climbing film front fell back slightly with a lapping action. Disintegration of the plugs often occurred as they passed the climbing film front. Both climbing and falling films could be formed simultaneously except at high wall temperatures. For example, at a wall temperature of 1000°C and a steam velocity of 3.1 m/s a jet of cold water of 4 g/s formed a wet patch in ~ 150 s which extended from about 50 mm above to about 20 mm below the jet. This test was continued for a further 500 s without progress of quenching in either direction, the surplus water flow being entrained out of the annulus. As the counterflow velocity was increased further only a climbing film was formed, and a gradual change in flow regime from plugging to annular flow occurred at the highest velocities (> 8 m/s). The general behaviour described above was typical of all tests (air, and steam with hot and cold water jets), but the detailed conditions at which changes occurred were different.

The stability of the observed phenomena require further comment. The quench front advance was typically irregular, and the plug formation appeared from ciné films to have a quasi-periodic character. It was also observed that the onset of the climbing film flow regime was unstable; the water film would travel perhaps ~ 50 mm upwards and then collapse, restoring falling film flow. Further tendencies to unstable behaviour were observed with steam counterflow and a subcooled water jet: at the onset of climbing film flow considerable water was held up in the annulus, but only around the wetted length of the rod. A crackling noise could be heard due to steam condensation as bubbling through the water occurred, and the water hold-up occasionally collapsed.

3.4 *Visual observations in two-phase counterflow*

In the two-phase counterflow experiments, the counterflow consisted of a dispersed flow of liquid and vapour in film boiling. A falling film progressed down the rod under all conditions, but receded slightly as intermittent surges in the counterflow were generated by the bottom flooding of the test section. A steady climbing film flow always occurred from the wet patch initiated by the jet flow. In all experiments the climbing film flow commenced before the water film spread downwards against the counterflow.

4. RESULTS

4.1 *Air-counterflow experiments*

The rewetting rates are shown plotted in figures 4–6. The first gives the results for a range of wall temperatures and flowrates and the latter two the detailed variations with wall temperature and flowrate.

Figure 4 shows clearly the retardation of the falling film (u^{-1} increases) as j_g increases, until at a counterflow velocity, j_{gf}, the film does not progress downwards. The retardation is greater at the lower flows (< 8 g/s) or wall temperatures greater than 700°C. For the lower temperatures, the falling film ceases for $j_g \gtrsim 5.5$ m/s which corresponds very nearly to the value of 6 m/s for the point of no net downflow determined independently for a cold annulus. It is important to observe that retardation of the falling film rewetting rate occurs well below this point, typically $j_g \gtrsim 1.0$ m/s at the highest temperatures or the lowest flows, this value increasing as these parameters are changed. The climbing films attain some slowly varying and apparently asymptotic velocity as j_g increases beyond 7 m/s, which is usually 1.2–1.4 times the falling film velocity without counterflow.

Climbing and falling films co-exist or overlap for a range of j_g except for $T_w > 700$°C with $\Gamma \leq 0.9$ g/s/cm when a stationary film exists. For $T_w = 900$°C and $\Gamma = 0.45$ g/s/cm a stationary film persists for $1 < j_g < 5$ m/s, the onset of the climbing film corresponding very nearly to the "flooding" countercurrent velocity for a cold rod.

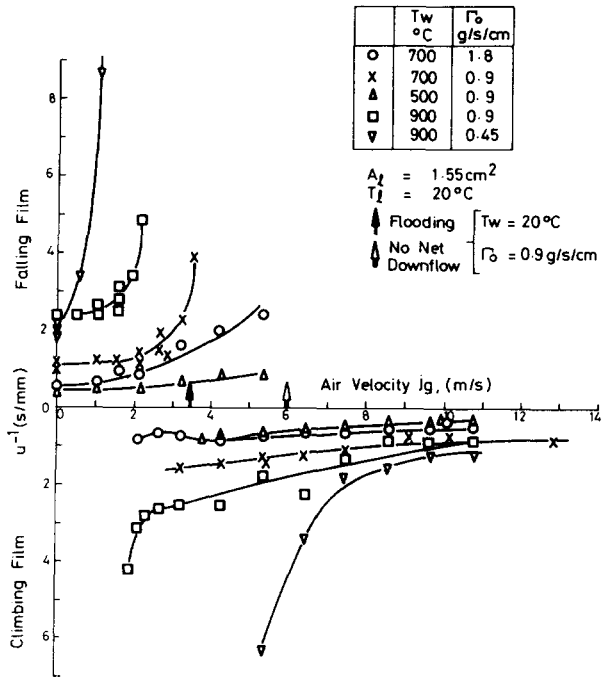

Figure 4. Effect of air counterflow on rewetting velocity.

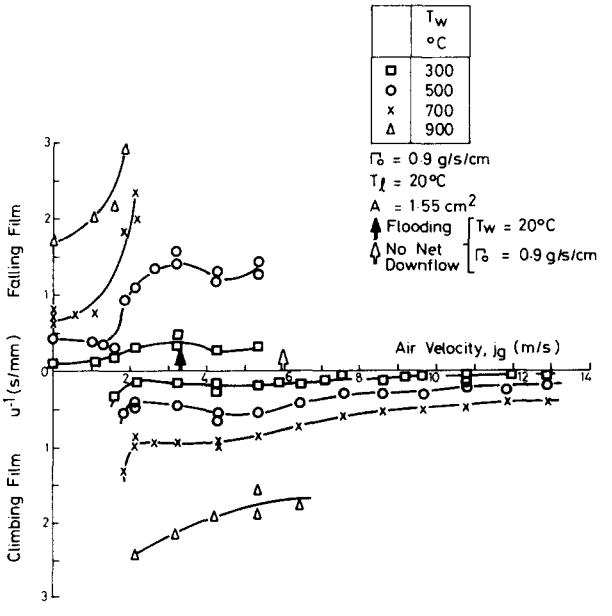

Figure 5. The effect of initial wall temperature with air counterflow.

Typical temperature traces are shown in figure 7: the surface 76 mm below the jet cools little before the arrival of the quench front whereas the surface 152 mm above the jet cools by ~ 100–200°C. The steep temperature drop associated with quenching also exhibits an interesting behaviour. The temperature falls progressively faster as quench velocity increases for both falling and climbing films.

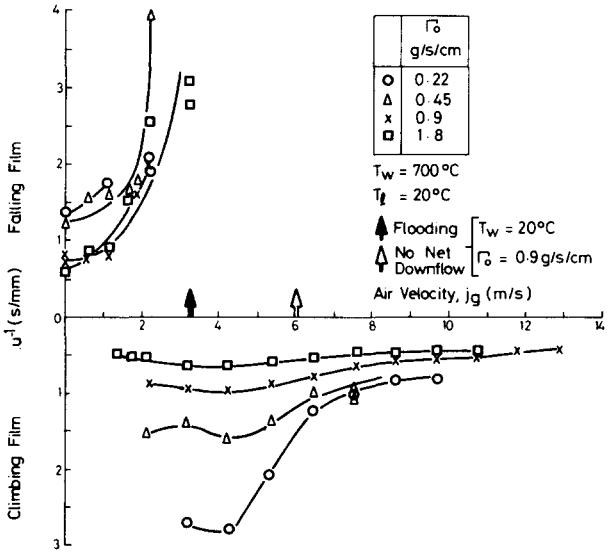

Figure 6. The effect of jet flowrate with air counterflow.

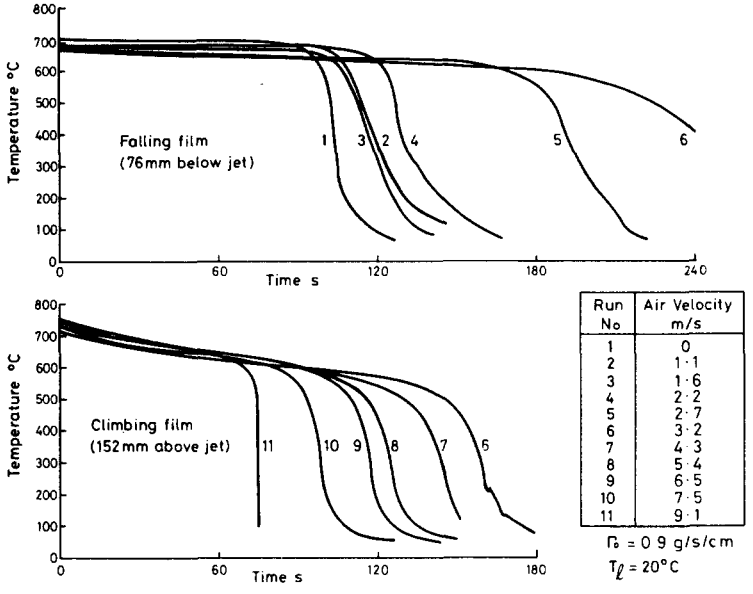

Figure 7. Temperature transients.

4.2 *Steam counterflow experiments*

The rewetting rate data for the steam-counterflow experiments are shown in figures 8 and 9 for inlet subcoolings of 80°C and 15°C respectively. The effect of a large subcooling in the inlet water jet was to produce a secondary minimum in inverse rewetting rate at a wall temperature of 700°C. During these experiments there was a hold-up of water in the annulus along the wetted length of the heater rod and condensation occurred as steam vented and bubbled through it. The application of higher steam flows were sufficient to raise the input water to saturation ensuring that no further condensation took place. A simple heat balance shows that for an inlet subcooling of 80°C and a flow rate 4 g/s a steam velocity of ≥ 6–8 m/s is needed to exceed this "condensation limited" region. This is in agreement with the observed rapid decrease in rewetting rate for $j_v > 7$ m/s.

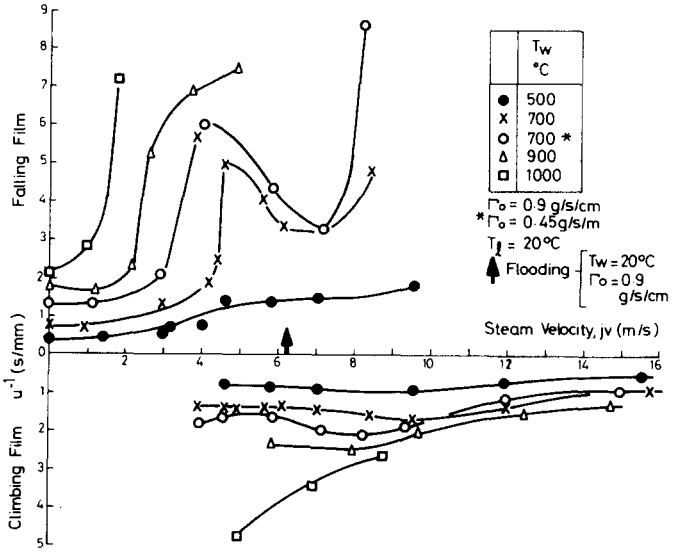

Figure 8. Steam counterflow data for a cold water jet.

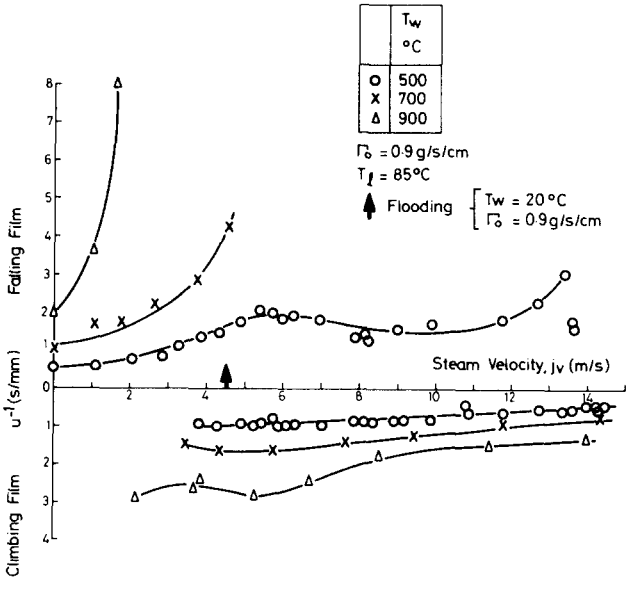

Figure 9. Steam counterflow data for a hot water jet.

During the steam experiments the flow from the condenser was noted for a wall temperature of 900°C and a cold water flow of 4 g/s. Some results are given in table 2 which show that nearly complete condensation of the steam occurs in the annulus only at the lowest counterflow velocities.

Table 2.

Steam velocity (m/s)	Steam flow (g/s)	Condenser flow (g/s)
1.2	0.1	0
2.6	0.22	0.05
3.7	0.31	0.14
4.9	0.41	0.25

This is reflected in less retardation of the falling film at a given counterflow than for the air or hot water/steam experiments, because condensation of even a small mass of steam causes a large reduction in vapour velocity. For the low subcooling of 15°C and a water flow rate of 4 g/s, a steam velocity of only 1.1 m/s is needed to raise the water to boiling point. Hence the film flow is always in the "interfacial shear" dominated region, and no secondary minimum due to condensation effects is observed in figure 9. Thus the general shape of the curves for steam counterflow with hot water are very like the air counterflow data because of the almost complete absence of interphase mass transfer in both cases.

The single-phase counterflow velocity, $j_{g,v}$, to produce a climbing film is from figures 4, 5, 6, 8 and 9, higher for steam than air by a factor of about 1.5. This corresponds to the square root of density ratio, and appears to be relatively insensitive to flow rate and wall temperature if $T_w \lesssim 700$°C. This suggests that the necessary conditions for the existence of a climbing film are hydrodynamically controlled; which implies that the counterflow dynamic head is the important parameter for creating climbing film flow. In the current experiments at atmospheric pressure the dynamic head at onset has a numerical value $\sim 2\ \mathrm{N/m^2}$. If the dynamic head at onset of climbing film flow is balanced against some hypothetical gravitational head in a thin film, then the maximum climbing film thickness is given by $\delta \sim \rho_{v,g} j_{v,g}^2 / 2\rho_L g \sim 0.2$ mm.

4.3 *Effects of annulus flow area and eccentricity*

The air counterflow experiments were extended to examine geometrical variations. The effect of doubling the annulus flow area to $\sim 2.9\ \mathrm{cm^2}$ was to eliminate the region of coexistence or overlapping of climbing and falling films (see figure 10a). This is attributed to the observed

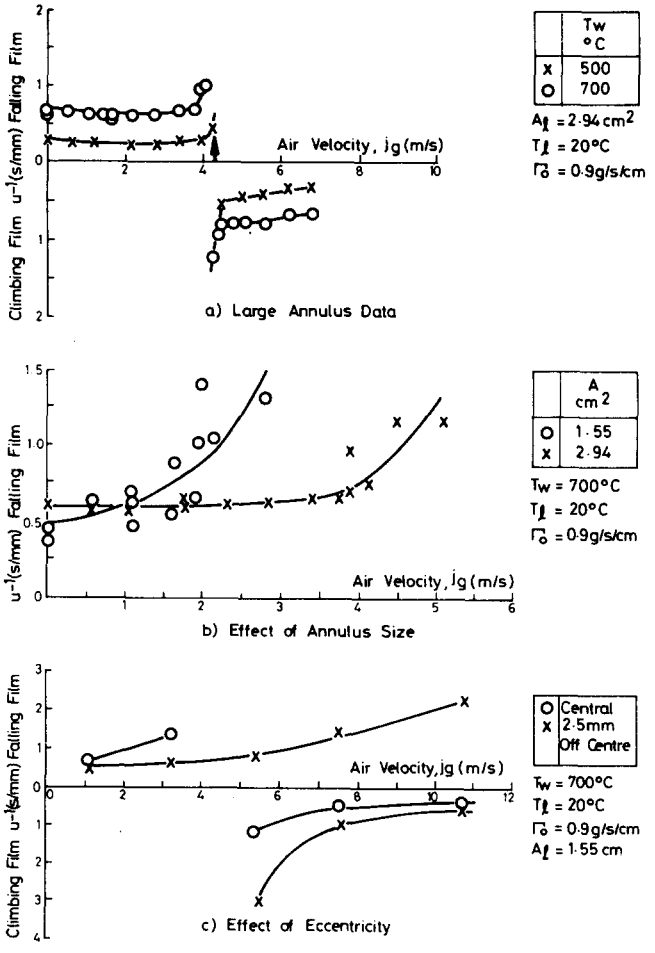

Figure 10. Effect of annulus size and eccentricity for air counterflow.

general absence of bridging with the wider annular gap, so that the climbing film flow could not be so readily supplied with water in intermittent upward plug flow. The change-over in film flow direction occurs at a velocity, j_g of ~ 4.4 m/s corresponding to that determined for no net downflow with a cold rod.

The effect of eccentricity was investigated by setting the rod 2.5 mm from the central position in the 1.55 cm^2 annulus (i.e. nearly touching one wall). The falling film proceeded down the side of the rod closest to the tube wall, the water bridging the gap, with the climbing film on the opposite side. This is presumably due to the counterflow bypassing the narrow gap. The effect of eccentricity (figure 10c) was to increase the counterflow needed to arrest the falling film by about a factor of three compared to the central rod results and to decrease climbing film quench velocity by about a factor of two at onset, the decrease becoming less at higher counterflow velocities (approx. 25% at 10 m/s).

It was found necessary to change both the heater and the silica tube during the course of the experiments because of failures. The results given in each figure were obtained with the same test section. It was found that despite rebuilding the test section to be nominally identical, the details of the results changed. It can be seen by comparing figures 4 and 5 which were obtained for different test sections, that the rewetting velocity for zero counterflow is different by up to 20%. Since the rewetting velocity is known to be a function of surface condition (Piggott & Porthouse 1973), changing the heater could have caused this effect. It can also be seen in figures 4 and 5 that the counterflow to arrest the falling film can be different by up to 50% at $T_w = 700$°C. The theory given in section 2 indicates that the effect of counterflow on falling film rewetting speed depends on the square of the flow area and so will be very sensitive to small changes in silica tube size, and the small eccentricities caused by heater bowing during the course of an experiment.

The observations and results given in this section, 4.3, all suggest that rod bundles will show very variable behaviour since they contain variations in subchannel flow dimensions and will be subjected to pin bowing.

4.4 *Two-phase counterflow experiments*

The results of these experiments are given in figures 11 and 12 and it should be noted that some of the water injected by the jet fell to the bottom of the annulus to add to that supplied independently. It can be seen from figure 11, which gives results for a 1.42 cm dia. stainless steel clad heater in an annulus of 1.2 cm^2 flow area, that the wet patch always spread both up and down the heater. The climbing film velocity under these conditions was typically twice that of the falling film. For comparison the rewetting data for a steam counterflow are replotted from

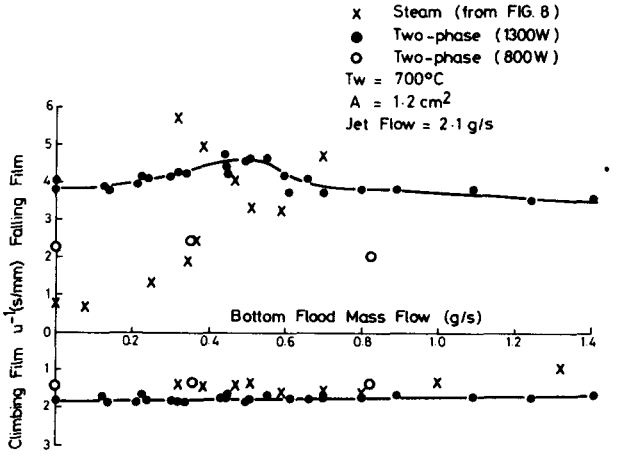

Fig 11. Two-phase counterflow results, and comparison with single-phase data.

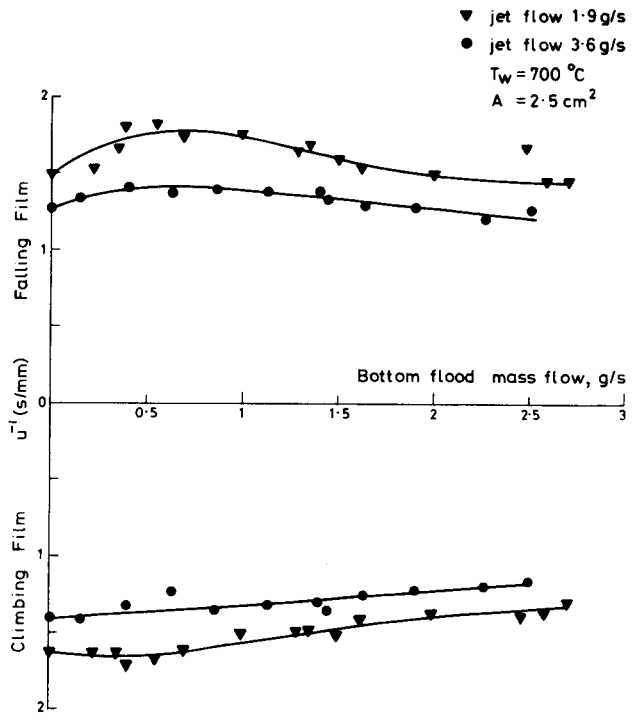

Figure 12. Two-phase counterflow results, the effect of jet flow.

figure 8, the steam velocities having been converted to mass flowrates. It can be seen that the climbing film velocities in single and two-phase counterflows were similar: whereas the two-phase falling film velocity was smaller at low bottom-flooding mass flows and corresponded to the single-phase value only above a bottom flood flow of 0.3 g/s.

In the above experiments the power required to maintain a constant wall temperature under conditions of counterflow in regions away from the jet (~ 1300 W) was greater than that needed under conditions of natural convection (~ 800 W). Experiments were performed at this lower power level and it can be seen from figure 11 that both falling and climbing film rewetting velocities were higher, consistent with the lower wall temperatures observed.

The effect of variations in jet flow was investigated with an inconel clad heater (1.59 cm dia). The heater power (~ 700 W) was sufficient to sustain a wall temperature of 700°C in conditions of natural convection. The results in figure 12 show that falling and climbing film rewetting velocities are similar and both increase with increasing jet flow.

4.5 *Pre-quench heat transfer*

Since the power input required to maintain the initial steady condition (~ 1000 W) was much larger than the power released during cooling (~ 200 W) any calculation of a heat transfer coefficient is very sensitive to the assumptions made about heat losses in the initial steady state. For this reason, the data has been presented as cooling rates. A cooling rate of 1°C/s on the heater thermocouples is equivalent to a heat flux of 1.22 w/cm^2 or 244 W for the entire heater. (Assuming a uniform radial temperature profile which is reasonable for slow cooling rates.)

Typical temperature transients were given in figure 7 for air counterflow experiments. The cooling rates are relatively constant up to the rapid fall associated with quenching, and these pre-quench cooling rates are shown plotted as a function of counterflow velocity in figure 13 for a jet mass flow of 4 g/s, variations with jet flow being small. The cooling rates both above and below the jet are shown.

Several points require comment. Firstly, it is clear that injecting water increases the heat removal, and this occurs mainly below the jet when a falling film quench occurs, and above

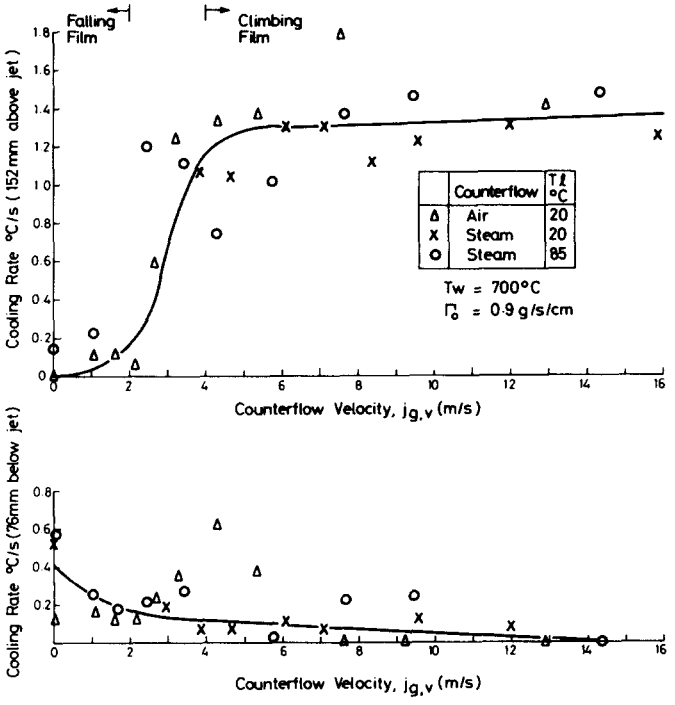

Figure 13. Pre-quench cooling rates for air and steam counterflows.

following flow reversal and the generation of a climbing film. Secondly, the air and steam counterflow data are in agreement, a result which suggests that condensation of the steam is not important. Thirdly, at high counterflow ($j_{g,v} > 4$ m/s) the additional cooling due to water injection is substantially independent of counterflow velocity. A consistent explanation for the increased heat transfer is the cooling to saturation temperature of the air and steam counterflows by the water injected into the annulus.

5. DISCUSSION AND COMPARISON WITH THEORY

5.1 *Comparison for present data with existing flooding correlations*

The available correlations for the disruption of film flow are for cold tubes. The present value of flooding (onset of film flow disruption) velocity, for an air counterflow and a cold rod, of 3.3 m/s is comparable with data from tubes. Based on the equivalent diameter of the annulus, and for an area of 1.5 cm^2 the correlation of Grolmes *et al.* (1974) for onset of increased pressure drop gives a value of j_{gf} of 3.4 m/s and the hanging film criterion of Wallis & Makkenchery (1974) a value of j_{gf} of 5.3 m/s. The onset of flooding in cold tests using steam and hot water injection occurred at $j_{vf} = 4.6$ m/s which is in accord with [6.2], i.e. dependent on square root of counterflow density. The value of j_{vf} for cold water injection was somewhat higher (6.2 m/s) due to condensation of some of the steam. The cold flooding tests with air counterflow showed that falling and climbing films coexist which is in qualitative agreement with the text-book definition of flooding in tubes as a transition region (Hewitt & Hall-Taylor 1970). Wallis & Makkenchery (1974), however, showed that for small diameter tubes the counterflow velocity required to produce upflow was twice that needed to prevent downflow.

5.2 *The effects of steam generation and condensation*

At low wall temperatures (≤ 500°C) the asymptote $u^{-1} \to \infty$ for the falling film coincides with the point of no net down-flow cold, whereas at higher wall temperatures the falling film rewetting rate is retarded or stopped at velocities ($\simeq 1$ m/s) well below that required to cause flooding when cold. An attempt is therefore made to account for the differences that occur as

wall temperature increases by considering the steam generated by the quenching process itself (i.e. stored heat release) and condensation of steam on the injected cold water. As an illustration, for the cold water/steam data from figure 8, steam velocities have been estimated from a simple heat balance,

$$j_v = j_{v0} + \frac{\rho cu(T_w - T_s) + Q - \gamma(\Gamma_0 \rho c_L \Delta T_s)}{\rho_v AL} \qquad [26]$$

where T_s is the saturation temperature, Q the electrical power input to the heater below the point of water injection, ρc the volumetric specific heat per unit length of heater and L the latent heat of vaporisation of water. The right hand term in the numerator of [26] is used to represent the heating of the water by condensation. The choice of the value of the multiplier, γ, will be dependent on the flow regime. At low counterflow velocities the water was in the form of an undisturbed film and γ was taken to be 0.1 consistent with condensation rates given by the correlation of Chun & Seban (1971). At higher steam velocities, $j_{v0} \geq 4$ m/s the flow regime changed to one in which the steam bubbled through the plug of water held in the annulus. The value of γ was therefore increased to account for increased water heating from a value of 0.1 at $j_{v0} = 4.3$ m/s to 1.0 at $j_{v0} = 7.3$ m/s near the flooding point.

Using this method the subcooled data from figure 8 are shown replotted in figure 14 which shows that most of the effects of wall temperature can be accounted for by considering steam generation and condensation. The air counterflow results were also treated by this method using a value of γ of 0.1 throughout and showed similar effects to the steam counterflow results. A rigorous calculation of steam generation and condensation will require further information on the effects of flow regime on condensation.

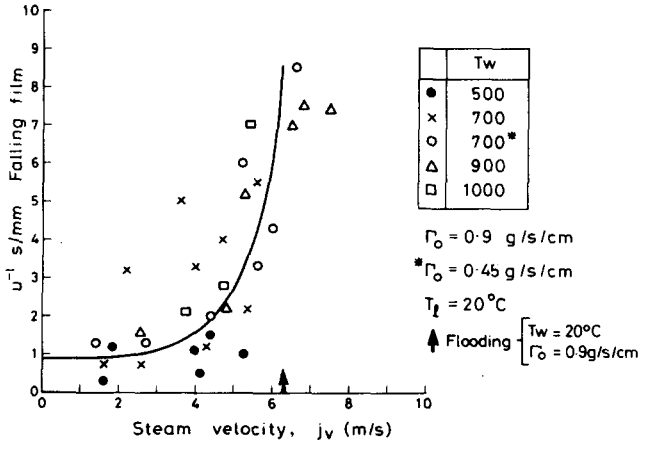

Figure 14. Data from figure 8 with steam velocity calculated from [26].

5.3 *Comparison of present data with interfacial shear theory*

Air and steam counterflow data for initial wall temperatures in the range 500–900°C were corrected to true steam velocities as described in 5.2 and are shown plotted in figure 15 in the manner suggested by [5]. The line through the data is

$$1 - \frac{u^*}{u_0^*} = 0.0021 \rho_{g,v} j_{g,v}^2 / \Gamma_0^{1/3}. \qquad [27]$$

The value of f implied by [27] is ~ 100 times the smooth tube value which is in accord with the observations of Anderson & Mantzouranis (1960). The air velocity at which falling film

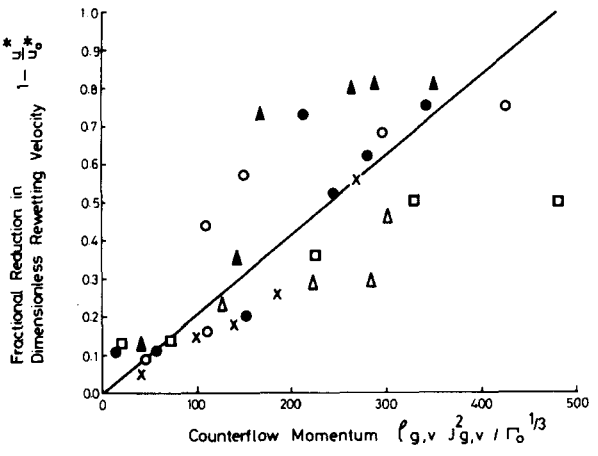

		Γ_0 g/s/cm	Tw °C
Steam	●	0·45	700
	▲	0·90	900
Air	x	0·90	700
	o	1·80	700
	Δ	0·90	900
	□	0·90	500

Figure 15. Comparison of interfacial shear analysis with air and steam counterflows data for 1.42 cm dia. rod in 1.55 cm^2 annulus.

rewetting ceases is, from figure 15, 6.1 m/s which agrees very closely with the velocity for no net down-flow from a cold test at the same water flow rate. The interfacial shear theory therefore gives a reasonable representation of the data which suggest that rewetting in the presence of counterflow is hydrodynamically controlled.

5.4 *Downcomer penetration studies*

Data on film flow rates as a function of counterflow velocity are given in downcomer penetration studies (Block 1975; Cudnik *et al.* 1975). In the experiments, with a counterflow of steam, water was poured between two parallel plates or concentric cylinders of width or circumference w, approx. 1 m and a gap spacing, s, between 10 and 50 mm. The results were presented by the authors in the conventional form of dimensionless countercurrent flux, J^*_c, vs dimensionless flow rate J^*_f. Where

$$J^*_c = (\rho j^2/(gw\rho_L))^{1/2} \qquad [28]$$

and

$$J^*_f = w^{1/2}\Gamma/\rho_L A(g)^{1/2} \simeq \Gamma/\rho_L s(gw)^{1/2}. \qquad [29]$$

To compare the downcomer penetration data with the simple interfacial shear theory of section 2, we need the value of $(\rho_v j_v^2/\Gamma_0^{1/3})$. Hence the data must be replotted as (c.f. [3]),

$$1-\Gamma/\Gamma_0 = CJ^{*2}_{vc}/J^{*1/3}_{f0} = C(\rho_v j_v^2 \Gamma_0^{-1/3})\left(\frac{s}{\rho_L^2}\right)^{1/3}\left(\frac{1}{wg}\right)^{5/6} \qquad [30]$$

so that there is equivalence with the interfacial shear theory when the slope,

$$C = f\frac{w^{5/6}}{4}\left(\frac{9g^{1/2}\rho_L}{\mu_L s}\right)^{1/3}. \qquad [31]$$

Replotted data are shown in figure 16: not only does this reduce the data to a common form but it can be seen that the trends are reasonably correlated by the present method, despite the data

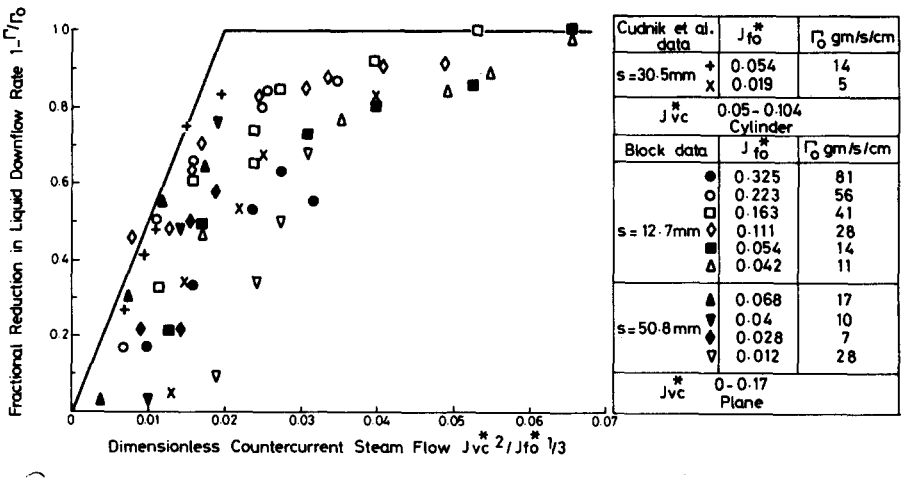

Figure 16. Comparison of interfacial shear analysis with steam-saturated water countercurrent flow data for plane and cylindrical surfaces.

scatter inherent in this type of experiment. The lines drawn represent the lower bound for downward water flow (as may be of interest for safety analysis) with $C = 50$ for $1-(\Gamma/\Gamma_0) < 1$. Thus, consistency of the interfacial shear model with other information is shown. The effect of water subcooling on the counterflow requires further study, since it evidently affects the flow regime and film flowrates.

5.5 *Wave dynamics and growth*

It has been observed that waves grow at the falling quench front until they bridge the gap between the silica tube and the heater to form a plug of water which is swept up the test section by the counterflow. Some measurements of wave growth taken from the ciné films are presented in figure 17. The waves appear to grow as $t^{1/2}$, in agreement with the Kapitza wave theory [18] but a value of $\delta_B = 0.004$ mm is needed to fit to data which is clearly too small. There is also a tendency for waves to grow faster for a higher initial wall temperature when the higher heat fluxes could result in greater film disruption. The preferential ease with which the waves grow at the front can be explained by the wavelength for neutral stability, λ_m, being comparable in scale to the fluid irregularities and ligaments observed at rewetting fronts (Duffey & Porthouse 1972).

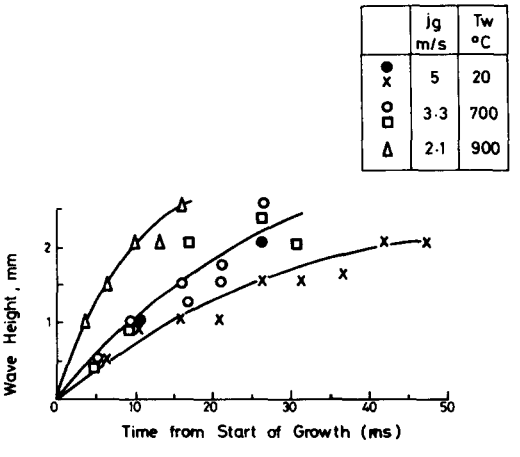

Figure 17. Preliminary estimates of wave growth.

6. CONCLUSIONS

Experiments on running a water film down a hot rod in an annulus showed that the falling film quench rate was significantly retarded by an air, steam or two-phase upflow, even before the point of flow reversal. Theoretical analysis of the film flow showed that a simple interfacial shear model although incapable of describing the observed wave dynamics, could correlate both the trends in the present data and that for downcomer penetration. It has been shown that, for wall temperatures up to 900°C, the falling film quench front ceases at a counterflow velocity which gives no net water downflow in a cold annulus, provided that steam generation and condensation are accounted for. Good agreement was obtained between the counterflow velocity at the onset of flooding in the present experiments and the value predicted by existing flooding correlations. Coexistent climbing and falling films occurred only at wall temperatures below 700°C: whereas at wall temperatures above 900°C a stable stationary film existed between the two regimes. The condensation of steam caused by injecting cold water was shown to affect the flow regime and to decrease the retardation of the falling film due to reduction of the steam velocity.

The physical mechanism for gross flow retardation and reversal was shown to be the growth of waves on the water film at the rewetting front. The waves bridged the annular gap and the plugs thus formed were accelerated upwards and the process repeated. A preliminary theoretical examination of the dynamics of finite-amplitude waves was carried out.

The pre-quench heat transfer showed significant spatial variations, being greatest in the direction of quench front propagation. Following film flow reversal, the cooling rate was found to be independent of the counterflow velocity, and identical trends and magnitudes occurred with both air and steam counterflows. A consistent explanation of the pre-quench heat transfer is that the steam or air counterflow is cooled to the saturation temperature by water injection.

Acknowledgement—This paper is published by permission of the Central Electricity Generating Board.

REFERENCES

ANDERSON, G. H. & MANTZOURANIS, B. G. 1960 Two-phase (gas–liquid) flow phenomena—I. Pressure drop and hold-up for two-phase flow in vertical tubes. *Chem. Engng Sci.* **12**, 109–126.

BARNETT, T. P. & KENYON, K. E. 1975 Recent advances in the studies of wind waves. *Rep. Prog. Phys.* **38**, 667–729.

BENJAMIN, T. B. 1957 Wave formation in laminar flow down an inclined plane. *J. Fluid Mech.* **2**, 554–574.

BLOCK, J. A. 1975 CREARE Downcomer Penetration Program. Presentation to 3rd Water Reactor Safety Information Meeting, Washington, 29 September.

CENTINBUDAKLAR, A. G. & JAMESON, G. J. 1969 The mechanism of flooding in vertical countercurrent two-phase flow. *Chem. Engng Sci.* **24**, 1669–1680.

CHAN, S. H. & GROLMES, M. A. 1975 Hydrodynamically controlled rewetting. *Nucl. Engng Design* **34**, 307–316.

CHU, K. J. & DUKLER, A. E. 1974 Statistical characteristics of thin, wavy films: I. Studies of the substrate and its wave structure. *A.I.Ch.E.Jl* **20**, 695–706.

CHUN, K. R. & SEBAN, R. A. 1971 Heat transfer to evaporating liquid films. *J. Heat Transfer* 391–396.

CUDNIK, R. A., FLANIGAN, L. J. & DENNING, R. S. 1975 Experimental studies on ECC delivery in a 1/15—scale transparent vessel model. Presentation to 3rd Water Reactor Safety Information Meeting, Washington, 30 September.

CUDNIK, R. A., FLANIGAN, L. J. & WOOTON, R. O. 1975 Studies of steam, water interactions in the downcomer of a 1/15—scale representation of a four-loop PWR. *Trans. A. N. S.* **21**, 337–339.

DUFFEY, R. B. & PORTHOUSE, D.T.C. 1972 Experiments on the cooling of high temperature surfaces by water jets and drops. Proc. CREST Specialist Meeting on ECC in LWRs, Munich, October.

DUFFEY, R. B. & PORTHOUSE, D.T.C. 1973 The physics of rewetting in water reactor emergency core cooling. *Nucl. Engng Design* **25**, 379–394.

DUKLER, A. E. 1972 Characterization, effects and modelling of the wavy gas–liquid interface. *Prog. Heat Mass Transfer* **6**, 207–234.

GOTTIFREDI, J. C. & JAMESON, G. J. 1970 The growth of short waves on liquid surfaces under the action of wind. *Proc. R. Soc.* **A319**, 273–397.

GROLMES, M. A., LAMBERT, G. A. & FAUSKE, H. K. 1974 Flooding in vertical tubes. Inst. Chem. Eng. Symp. Series No. 38, *Proc. Symp. Multiphase Flow Systems*, Glasgow, Paper A4.

GUERRERO, H. N. & LOWE, P. A. 1974 Exploratory single-tube top flooding gravity-feed heat transfer tests. *Trans. A. N. S.* **18**, 234.

HANRATTY, T. J. & HERSHMAN, A. 1961 Initiation of roll waves. *A. I. Ch.E.Jl* **7**, 488–497.

HEWITT, G. F. & HALL-TAYLOR, N. S. 1970 *Annular Two-Phase Flow*. Pergamon, Oxford.

HEWITT, G. F. & WALLIS, G. B. 1963 Flooding and associated phenomena in falling film flow in a tube. UKAEA Report AERE–R4022.

ISHII, M. & GROLMES, M. A. 1975 Inception criteria for droplet entrainment in two-phase concurrent film flow. *A.I.Ch.E.Jl* **21**, 308–318.

JEFFREYS, H. 1925*a* On the formation of water waves by wind. *Proc. R. Soc.* **107**, 189–205.

JEFFREYS, H. 1925*b* On the formation of water waves by wind (second paper). *Proc. R. Soc.* A. **110**, 241–247.

LACEY, P. M. C., HEWITT, G. F. & COLLIER, J. G. 1962 *Proc. Inst. Mech. Engrs Symp.* on two-phase fluid flow, 1–12.

LAMB, H. 1945 *Hydrodynamics*, pp. 625–628. Dover, New York.

LANDAU, L. D. & LIFSCHITZ, E. M. 1959 *Course of Theoretical Physics*, Vol. 6, *Fluid Mechanics*, pp. 396–398. Pergamon, Oxford.

LEE, J. 1969 Kapitza's method of film flow description. *Chem. Engng Sci.* **24**, 1309–1319.

MAYER, E. 1961 Theory of liquid atomization in high velocity gas streams. *A.R.S. Jl* **31**, 1783–1785.

MILES, J. W. 1957 On the generation of waves by shear flows. *J. Fluid Mech.* **3**, 185–204.

MILES, J. W. 1967 On the generation of surface waves by shear flows, Part 5. *J. Fluid Mech.* **30**, 163–175.

MIYA, M., WOODMANSEE, D. E. & HANRATTY, T. J. 1971 A model for roll waves in gas–liquid flow. *Chem. Engng Sci.* **26**, 1915–1931.

NAFF, S. A. & WHITBECK, J. F. 1973 Steady state investigation of entrainment and countercurrent flow in small vessels. *Am. Nucl. Soc.*, Topical Meeting on Water Reactor Safety, Salt Lake City, CONF–730304, 212–220.

NICKLIN, D. J. & DAVIDSON, J. F. 1962 The onset of instability in two-phase plug flow. *Proc. Inst. Mech. Engrs Symp.* on Two-phase Fluid Flow, 29–34.

PEARSON, K. G., PIGGOTT, B. D. G. & DUFFEY, R. B. 1977 The effect of thermal diffusion from fuel pellets on rewetting of overheated water reactor pins. *Nucl. Engng Design* **41**, 165–173.

PIGGOTT, B. D. G. & DUFFEY, R. B. 1975 The quenching of irradiated fuel pins. *Nucl. Engng Design* **32**, 182–190.

PIGGOTT, B. D. G. & PORTHOUSE, D. T. C. 1973 Water reactor emergency core cooling: the effect of pressure, subcooling and surface condition on the rewetting of hot surfaces. CEGB Report RD/B/N2692.

PIGGOTT, B. D. G. & PORTHOUSE, D. T. C. 1975 A correlation of rewetting data. *Nucl. Engng Design* **32**, 171–181.

PIGGOTT, B. D. G., WHITE, E. P. & DUFFEY, R. B. 1976 Wetting delay due to film and transition boiling on hot surfaces. *Nucl. Engng Design* **36**, 169–181.

SEMERIA, R. & MARTINET, B. 1965 Califaction spots on a heating wall, temperature distribution

and resorption. Symp. on Boiling Heat Transfer in Steam Generating Units, *Proc. Inst. Mech. Engns* **180**, 192–205.

SHEARER, C. J. & DAVIDSON, J. F. 1965 The investigation of a standing wave due to gas blowing upwards over a liquid film: its relation to flooding in wetted wall columns. *J. Fluid Mech.* **22**, 321–335.

SHIRES, G. L. PICKERING, A. R. & BLACKER, P. T. 1964 Film cooling of vertical fuel rods. UKAEA Report AEEW-R-343.

TELLES, A. S. & DUKLER, A. E. 1970 Statistical characteristics of thin, vertical, wavy, liquid films. IEC Fundamentals **9**, 412–421.

THEOFANOUS, T. G., DI MONTE, M. & PATEL, P. D. 1976 Incoherency effects in clad relocation dynamics for LMFBR CDA analyses. *Nucl. Engng Design* **36**, 59–67.

UEDA, T., & TANAKA, T. 1974 Studies of liquid film flow in two-phase annular and annular-mist flow regions. (Part 1, Downflow in a vertical tube). *Bull. J.S.M.E.*, **17**, 603–613.

UEDA, T. & NOSE, S., 1974 Studies of liquid film flow in two-phase annular and annular-mist flow regions. (Part 1, Upflow in a vertical tube). *Bull. J.S.M.E.*, **17**, 603–613.

VAN ROSSUM, J. J. 1959 Experimental investigation of horizontal liquid films. *Chem. Engng Sci.* **11**, 35–52.

WALLIS, G. B. 1969 *One-dimensional Two-phase Flow.* McGraw Hill, New York.

WALLIS, G. B. & DOBSON, J. E. 1973 The onset of slugging in horizontal stratified air–water flow. *Int. J. Multiphase Flow* **1**, 173–193.

WALLIS, G. B. & MAKKENCHERY, S. 1974 The hanging film phenomenon in vertical annular two-phase flow. *J. Fluids Engng* **96**, 297–298.

WHALLEY, P. B., HUTCHINSON, P. & HEWITT, G. F., 1974, The calculation of critical heat flux in forced convection boiling. Fifth Internationnal Heat Transfer Conference, Tokyo, **4**, 290–294.

YIH, C. S. 1963 Stability of Liquid Flows down an inclined plane. *Physics Fluids* **6**, 321–334.

YOSHIOKA, K. & HASEGAWA, S. 1970 A correlation of displacement velocity of liquid film boundary formed on a heated vertical surface in emergency cooling. *J. Nucl. Sci. Tech.* **7**, 418–425.

YU, S. K. W., FARMER, P. R. & CONEY, M. W. E. 1977 Methods and correlations for the prediction of quenching rates on hot surfaces. *Int. J. Multiphase Flow* **3**, 415–443.